JOURNAL OF MATERIALS SCIENCE **38** (2003) 1107–1115

Ultrasonic determination of the elastic and nonlinear acoustic properties of transition-metal carbide ceramics: TiC and TaC

S. P. DODD
Department of Physics, University of Bath, Bath BA2 7AY, UK

M. CANKURTARAN
Department of Physics, Hacettepe University, Beytepe, 06532 Ankara, Turkey
E-mail: cankur@hacettepe.edu.tr

B. JAMES
DSTL-Chertsey (Armour Group), Chobham Lane, Chertsey, Surrey KT16 OEE, UK

Pulse-echo overlap measurements of ultrasonic wave velocity have been used to determine the elastic stiffness moduli and related elastic properties of ceramic transition-metal carbides TiC and TaC as functions of temperature in the range 135–295 K and hydrostatic pressure up to 0.2 GPa at room temperature. The carbon concentration of each ceramic has been determined using an oxidation method: the carbon-to-metal atomic ratios are both 0.98. In general, the values determined for the adiabatic bulk modulus (B^S), shear stiffness (μ), Young's modulus (E), Poisson's ratio (σ) and acoustic Debye temperature (Θ_D) for the TiC and TaC ceramics agree well with the experimental values determined previously. The temperature dependences of the longitudinal stiffness (C_L) and shear stiffness measured for both ceramics show normal behaviour and can be approximated by a conventional model for vibrational anharmonicity. Both the bulk and Young's moduli of the ceramics increase with decreasing temperature and do not show any unusual effects. The results of measurements of the effects of hydrostatic pressure on the ultrasonic wave velocity have been used to determine the hydrostatic pressure derivatives of elastic stiffnesses and the acoustic-mode Grüneisen parameters. The values determined at 295 K for the hydrostatic pressure derivatives $(\partial C_L/\partial P)_{P=0}$, $(\partial \mu/\partial P)_{P=0}$ and $(\partial B^S/\partial P)_{P=0}$ for TiC and TaC ceramics are positive and typical for a stiff solid. The adiabatic bulk modulus B^S and its hydrostatic pressure derivative $(\partial B^S/\partial P)_{P=0}$ of TiC are in good agreement with the results of recent high pressure X-ray diffraction measurements and theoretical calculations. The longitudinal (γ_L), shear (γ_S) and mean (γ^{el}) acoustic-mode Grüneisen parameters of TiC and TaC ceramics are positive: the zone-centre acoustic phonons stiffen under pressure. The shear γ_S is much smaller than the longitudinal γ_L. The relatively larger values estimated for the thermal Grüneisen parameter γ^{th} in comparison to γ^{el} for the TiC and TaC ceramics indicate that the optical phonons have larger Grüneisen parameters. Hence knowledge of the elastic and nonlinear acoustic properties sheds light on the thermal properties of ceramic TiC and TaC.

1. Introduction

Transition-metal carbides (TMCs) are interesting for both fundamental studies and technological applications. The TMCs studied here: TiC and TaC, have a range of properties, which are utilised for technological purposes. These include great hardness, high chemical stability and resistance to corrosion, high melting point (TaC has the highest melting point of any known material at 3983°C), good mechanical stability and brittle-to-ductile transitions at high temperatures [1]. For example, these carbides are extensively used as hard constituents in metal matrix composites (hard-metals) and in the forming of layers (coatings) on cutting tools. Metallic behaviour in their electrical, magnetic and optical properties has also been found [1]. According to Williams [2], a potential electrical application for these carbides is for interconnects in very large-scale integrated circuits.

Each transition-metal carbide (or monocarbide) used in the present ultrasonic study crystallizes in the NaCl (B-1) structure (space group: $Fm\bar{3}m$), with 2 atoms per unit cell [1]. One way to visualise this structure is a face centred cubic (fcc) metal lattice with the octahedral interstitial sites filled by carbon atoms; when all the

octahedral sites are filled, the transition metal to carbon atom ratio is one-to-one, and the compound is classed as stoichiometric. In practice, this stoichiometry is seldom reached and the carbides are then classed as substoichiometric, but retain their NaCl structure over a wide range of carbon concentrations [1], which results in carbon vacancies at the interstitial sites. The corresponding concentration of carbon vacancies ranges from 2–3% to 50% in these monocarbides [3]. The carbon vacancies are randomly distributed in the carbon sublattice of TMCs and are recognised as scattering centres for electrons and phonons. It has also been suggested by Williams [3] that disordered-to-ordered phase transitions, which occur in some TMCs at different metal/carbon ratios, means that the structures are metastable. Due to a mixture of metallic, covalent and ionic bonding in transition-metal carbides, Williams [4] has described these compounds as "metallic ceramics".

Despite the technological importance of TMCs understanding of the elastic and nonlinear acoustic properties of their ceramic form is sparse. For design purposes the elastic behaviour of transition-metal carbide ceramics must be evaluated as functions of temperature and pressure. Previously the elastic moduli (i.e. Young's modulus (E) and shear modulus (μ)) of ceramic samples of TMCs were measured at room temperature using different measurement techniques: composite resonator [5], resonance pulse method [6], sonic resonance method [7] and free vibration method [8]. Recently, Kral *et al*. [9] compiled a large number of room temperature Young's modulus and Poisson's ratio (σ) values for TMCs samples with varying compositions and porosity, but the data scatter was large. Measurements of the Young's modulus of polycrystalline $TiC_{0.84}$ as a function of temperature in the range from 20 to 1600°C were reported in the literature [5], but very little has been published on the low temperature elastic properties of TMCs. Chang and Graham [10] used a pulsed ultrasonic phase comparison technique to measure the second order elastic constants (SOECs) of single-crystal $TiC_{0.91}$ in the temperature range from 4.2 to 298 K. However, no work on the effects of pressure on the elastic behaviour of transition-metal carbide ceramics is available in the literature.

The present high pressure ultrasonic study of the elastic and nonlinear acoustic properties of ceramic TiC and TaC has been largely motivated by the need for accurate measurements of the effects of hydrostatic pressure on the velocities of longitudinal and shear ultrasonic waves propagated in these ceramics. These measurements are essential for design purposes in engineering applications and scientific investigations of the dynamic response of the material to applied pressure or shock waves. To assess the nonlinear acoustic properties of ceramic TiC and TaC, ultrasonic wave velocities have been measured as a function of hydrostatic pressure up to 0.2 GPa at room temperature; ultrasonic wave velocity measurements on these ceramics have been extended from room temperature down to 135 K. The outcome of this experimental work has been the determination of the technological elastic stiffness moduli and related elastic properties of these ceramics and how they vary with temperature and hydrostatic pressure. The elastic stiffnesses of a material determine the slopes of the acoustic phonon dispersion curves in the long-wavelength limit; their hydrostatic pressure dependences provide information on the shift of the mode energies with compression and hence on the anharmonicity of zone-centre acoustic phonons. The present results provide intriguing physical insight into the elastic and nonlinear acoustic properties and in turn on the thermal properties of ceramic TiC and TaC.

2. Experimental procedures

The TiC and TaC ceramics used in this work were supplied by Testbourne (U.S.A.). The ceramics were prepared by using a hot-pressing technique. X-ray studies of each ceramic showed that there was no preferred orientation and no detectable secondary phases were evident. An electron microprobe analysis revealed the presence of a small proportion of oxygen: 1.62 at.% and 0.011 at.% in the TiC and TaC ceramics, respectively. Spectroscopic analysis of the starting powders used in the fabrication of these ceramics revealed the presence of very small amounts of impurities. The TiC powders contained, by weight, <0.01% Ca and <0.03% Fe, while the TaC powders contained 0.005% Al, <0.001% Ca, 0.01% Fe, 0.02% Nb and 0.01% Si.

The carbon deficiency in transition-metal carbides affects their physical properties including the elastic properties [1, 5, 10, 11], hence it is important to determine the carbon concentration of each carbide ceramic. A number of non-destructive methods can be used to determine the carbon concentration in these carbides, but care has to be taken when employing them. In the case of carbide samples with measurable impurities and defect microstructures, non-destructive methods are inappropriate to determine the carbon concentration. To determine the carbon concentrations of ceramic TiC and TaC an oxidation method, similar to that discussed by Toth [1], was employed in this work. Ceramic offcuts from the same block as the ultrasonic samples were pulverised to produce the carbide powders used in the oxidation experiments. Carbide powders were then converted to oxides. Oxidation experiments were performed in still air with each powdered sample placed on a platinum foil lined alumina boat inside a tube furnace, capable of reaching 1200°C; the weight changes were monitored periodically until no further changes were witnessed. The results of these experiments including the predicted oxidation reactions (given by [12, 13]), oxidation temperatures and duration times for full oxidation of these carbides are given in Table I. The carbon concentration (x) of each carbide sample was estimated using

$$x = \frac{M_{\text{oxide}}(W_{\text{C}}/W_{\text{oxide}}) - M_{\text{TM}}}{M_{\text{Cbn}}}, \qquad (1)$$

where M_{oxide}, M_{TM}, and M_{Cbn} are the molar (or atomic) masses of the transition-metal oxide compound, transition metal, and carbon, respectively; W_{C} and W_{oxide} are the measured weights of the carbide powders before and after oxidation, respectively. The mean carbon concentration was found to be 0.98 ± 0.06 and

TABLE I Experimental parameters for the oxidation experiments: predicted oxide compounds produced in the oxidation reactions, oxidation temperatures and duration times for full oxidation. Oxidation reactions and temperatures were taken from the references given. Results of the oxidation of TiC and TaC powders are given as carbide powder weights before and after oxidation

Results of oxidation experiments		
Material	TiC	TaC
Experimental parameters		
Oxidation reaction	$TiC \Rightarrow TiO_2$	$TaC \Rightarrow Ta_2O_5$
Temperature	900°C	800°C
Duration	∼4 days	∼2 days
Reference	[12]	[13]
Results		
Weight of carbide powders (grams)		
Powder 1	0.0400 ± 0.0002	0.0789 ± 0.0002
Powder 2	0.0315 ± 0.0003	0.0407 ± 0.0003
Measured weight after oxidation (grams)		
Powder 1	0.0540 ± 0.0006	0.0906 ± 0.0003
Powder 2	0.0419 ± 0.0003	0.0466 ± 0.0003
Estimated carbon concentration (x)		
Powder 1	0.94 ± 0.06	0.95 ± 0.07
Powder 2	1.01 ± 0.06	1.00 ± 0.16
Average	0.98 ± 0.06	0.98 ± 0.12

0.98 ± 0.12 for TiC and TaC, respectively, showing that the samples were close to stoichiometry. Hereinafter, the samples will be referred to using the estimated concentrations: $TiC_{0.98}$ and $TaC_{0.98}$. Some assumptions were made to arrive at these estimations. These are: the weight influences due to impurities were negligible, no transition-metal oxide was present in the powder before oxidation, no transition metal or metal oxide was lost during the oxidation experiments, and the final oxide compounds corresponded to those suggested in the literature. The assumption that no transition metal or metal oxide was lost during the reaction is valid, because the vapour pressures are negligible at the reaction temperatures given in Table I, i.e. the vapour pressures for Ti and Ta are 3×10^{-9} and 3×10^{-27} Pa, respectively [14]. Similarly, the vapour pressures of the transition-metal oxides are 1 Pa for TiO_2 at 1780°C and 1 Pa for Ta_2O_5 at 2000°C (data taken from http://www.jubochina.com), values that should be significantly lower at the oxidation temperatures used in this study. The last assumption was strengthened by the results of an X-ray study on powder 1 of each monocarbide and revealed that the predicted oxide compounds were in fact produced.

To further characterise the fundamental properties of the TiC and TaC ceramics, electrical resistivity has been measured in the temperature range from 300 to 1300 K, in an atmosphere of flowing dry nitrogen. A ceramic bar with approximate dimensions $1.5 \times 1.5 \times 10$ mm was cut from the same block as the ultrasonic sample. To measure the electrical resistance of the bar sample, a standard four-point probe method was used, and the samples were supplied with dc current between 50 and 100 mA. The main error (about 2%) in resistance was that incurred in determining the contact separation. Errors in the resistivity calculations appearing because of contact placement and sample dimensions

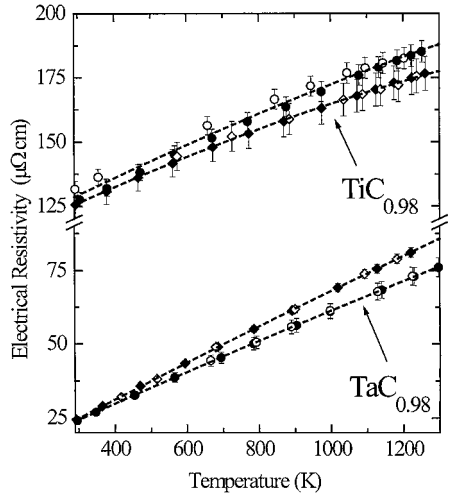

Figure 1 Temperature dependence of the electrical resistivity for $TiC_{0.98}$ and $TaC_{0.98}$ ceramics, measured using a four-point probe dc technique. The circles (diamonds) correspond to sample 1 (sample 2). Filled (open) symbols refer to measurements made with increasing (decreasing) temperature. The dashed lines are second order polynomial fits to the experimental data.

were tested by a Poisson equation calculation [15], and were found to be negligible. Other errors such as thermal voltages were removed by taking forward and reverse current measurements. Averaging the results of room-temperature resistivity measurements on two bar samples of each ceramic material resulted in values of 126 ± 4 and 24 ± 1 $\mu\Omega$cm for $TiC_{0.98}$ and $TaC_{0.98}$, respectively. However, these resistivity values are affected by the defect microstructure of the samples and do not agree well with previous studies on polycrystalline samples [16]. The lack of sample characterisation (i.e. impurities, carbon content, porosity) in previous studies on electrical properties of TiC and TaC makes it difficult to compare the present data with those available in the literature; consequently, a large variation in the results of electrical resistivity measurements is produced [16, 17]. Both the $TiC_{0.98}$ and $TaC_{0.98}$ ceramics show metallic-like electrical behaviour with increasing temperature (Fig. 1). The average temperature coefficients of resistivity for the $TiC_{0.98}$ and $TaC_{0.98}$ ceramics, evaluated at room temperature, are 66 ± 19 and 60 ± 2 nΩcmK^{-1}, respectively.

The mass density (ρ) of ultrasonic samples was measured by Archimedes' method using distilled water as a flotation fluid (Table II). The density measurements revealed that the ceramics had a porous microstructure, and this was later confirmed by SEM analysis. To obtain the theoretical density and hence to determine the porosity for each of the carbide ceramics, data by Storms [12] on the lattice parameters as a function of carbon composition were used. The correct lattice parameters corresponding to the mean carbon concentrations (shown in Table I) were used to calculate the unit cell volumes, which in turn enabled a theoretical density to be computed for that carbon concentration. The results of these calculations to determine the theoretical density of each carbide, and hence its porosity percentage, are shown in Table II. An ultrasonic sample, in the shape of a parallelepiped with approximate

TABLE II Sample mass densities, "theoretical" densities, porosity percentages, averaged ultrasound velocities, adiabatic elastic moduli and their hydrostatic pressure derivatives, and acoustic-mode Grüneisen parameters for the ceramic transition-metal carbides at 295 K. Ultrasonic wave velocities and elastic moduli have not been corrected for porosity

Material	$TiC_{0.98}$	$TaC_{0.98}$
Mass density (kg m^{-3})	4495 ± 4	12788 ± 50
Theoretical density (kg m^{-3})	4886 ± 293	14478 ± 1737
Porosity (%)	8.0 ± 0.5	11.7 ± 1.4
V_L (ms^{-1})	9429 ± 40	6232 ± 10
V_S (ms^{-1})	5856 ± 24	3744 ± 13
C_L (GPa)	399 ± 2	496 ± 2
μ (GPa)	154 ± 1	179 ± 1
B^S (GPa)	193 ± 2	257 ± 2
E (GPa)	365 ± 4	435 ± 3
σ	0.186 ± 0.002	0.218 ± 0.002
Θ_D (K)	862 ± 6	531 ± 3
$(\partial C_L/\partial P)_{P=0}$	6.32 ± 0.26	7.12 ± 0.24
$(\partial \mu/\partial P)_{P=0}$	1.83 ± 0.20	1.61 ± 0.06
$(\partial\ B^S/\partial P)_{P=0}$	3.88 ± 0.35	4.97 ± 0.25
γ_L	1.37 ± 0.07	1.68 ± 0.07
γ_S	0.98 ± 0.11	0.99 ± 0.04
γ^{el}	1.11 ± 0.08	1.22 ± 0.04

dimensions $10 \times 8 \times 8$ mm, which was large enough for precision measurements of ultrasonic wave velocities, was cut and polished with a pair of faces, flat to surface irregularities of about 3 μm and parallel to better than 10^{-3} rad.

To generate and detect ultrasonic pulses, X- or Y-cut (for longitudinal and shear waves, respectively) 10-MHz quartz transducers, operated in the frequency range 10–50 MHz, were bonded to the specimen using Nonaq stopcock grease for low temperature experiments. Dow resin was used as bonding material for high-pressure experiments. Ultrasonic pulse transit times were measured using a pulse-echo overlap system [18], capable of a resolution of velocity changes to 1 part in 10^5 and particularly well suited to determination of pressure- or temperature-induced changes in velocity. A correction was applied to the ultrasonic wave velocity for multiple reflections at the sample transducer interface [19]. The temperature dependence of ultrasound velocity was measured in the temperature range 135–295 K using a closed-cycle cryostat. At lower temperatures, thermal expansion differences between sample, bond and transducer caused the ultrasonic signal to be lost; a number of bonding agents were tried, but none gave satisfactory results. The dependence of ultrasonic wave velocity upon hydrostatic pressure was measured at room temperature (295 K). Hydrostatic pressure up to 0.2 GPa was applied in a piston-and-cylinder apparatus using silicone oil as the pressure-transmitting medium. Pressure was measured using a pre-calibrated manganin resistance gauge. Pressure-induced changes in the sample dimensions were accounted for by using the "natural velocity (W)" technique [20].

3. Temperature dependence of the elastic stiffness moduli

The velocities of longitudinal (V_L) and shear (V_S) ultrasonic waves propagated in the $TiC_{0.98}$ and $TaC_{0.98}$ ceramic samples at room temperature (295 K) are given in Table II. Each of these small grained polycrystalline ceramics can be treated as an isotropic material, which has two independent elastic stiffness moduli $C_L(= \rho V_L^2)$ and $\mu(= \rho V_S^2)$, because the ultrasonic wavelength is much larger than the average grain size. The elastic anisotropy was checked by measuring both longitudinal and shear wave velocities in the sample at room temperature for three orthogonal wave propagation directions: each ceramic was found to be elastically isotropic. $TiC_{0.98}$ had the larger discrepancies in the measured sets of longitudinal and shear ultrasonic velocities, but these discrepancies only amounted to differences of 1% in the longitudinal and shear wave velocities. The longitudinal C_L and shear μ elastic stiffnesses, adiabatic bulk modulus B^S, Young's modulus E, Poisson's ratio σ, and acoustic Debye temperature Θ_D, determined at room temperature and atmospheric pressure, from the ultrasonic velocity data and sample density, are summarised in Table II. The average longitudinal and shear wave velocities obtained from the data measured to assess the elastic isotropy of the samples have been used in the calculation of these elastic properties. The relatively large bulk modulus is consistent with the strong interatomic bonding in these carbides [21].

The presence of pores in ceramic samples leads to reductions in the measured ultrasonic wave velocities (and hence the elastic stiffness moduli). To enable a meaningful comparison between the present results and the elastic property data existing in the literature, it is important to establish the ultrasonic velocities that correspond to the non-porous matrix of each carbide ceramic used in this work. This has been achieved by applying multiple-scattering theory developed [22] for ultrasonic propagation in two-phase materials consisting of spherical inclusions in a matrix and extended [23] self-consistently to a porous medium (when the scatterer is a void). This theory is applicable to polycrystalline samples with porosity up to 30%. Using the measured porosity and solving numerically the multiple-scattering equations in the low-frequency regime, we have calculated the ultrasonic wave velocity values and hence the elastic stiffness moduli for the non-porous matrices of the $TiC_{0.98}$ and $TaC_{0.98}$ ceramics. The elastic moduli (C_L, μ, B^S and E) and the acoustic Debye temperature (Θ_D) for both carbide ceramics are increased significantly by this correction for the effects of porosity (Table III); Poisson's ratio (σ) is affected only slightly. The problem of porosity in polycrystalline samples of transition-metal carbides and its effect on their elastic properties has previously been encountered in studies on samples of TiC [24, 25], and TaC [6, 8]. The elastic moduli measured in these other studies were corrected for the effects of porosity by extrapolation of porosity dependent data to zero porosity. A compilation of the elastic moduli data for nearly stoichiometric TiC and TaCceramics presented in previous studies (but only those where the carbon concentration was specified) is also given in Table III. There is a general agreement between the present and previous data where it exists, but the small discrepancies may be a result of variation in microstructure (i.e. carbon

TABLE III Comparison of the available elastic data on nearly stoichiometric TiC and TaC ceramics and single crystals with the porosity corrected values found in the present study. The symbol (*) denotes Hill averages for single-crystal (s) elastic constants, (hp) and (sint) denote porosity corrected elastic properties of hot-pressed and sintered ceramic samples, respectively, and (–) means sample preparation method not given

Material		Type	E (GPa)	μ (GPa)	B (GPa)	σ	Θ_D (K)	Reference
	$TiC_{0.98}$	hp	436 ± 26	184 ± 11	233 ± 14	0.187 ± 0.010	929 ± 56	This work
	$TiC_{0.84}$	–	400	164	233	0.25	884	[5]
Titanium carbide	$TiC_{0.91}$	s,*	449	188	242	0.191		[10]
	TiC	s,*	437	182	242	0.200		[26]
	$TiC_{0.95}$	s,*	462	193	253			[11]
	$TiC_{\sim 1.0}$	sint	460	190	232	0.17	946	[25]
	$TaC_{0.98}$	hp	567 ± 68	234 ± 27	332 ± 39	0.215 ± 0.020	593 ± 71	This work
	$TaC_{0.97}$	s,*	539	217	343			[28]
Tantalum carbide	$TaC_{0.99}$	sint	552	227	317	0.21		[6]
	$TaC_{0.99}$	hp	546	226		0.21		[7]
	$TaC_{0.994}$	–	537	216	344	0.24		[8]
	$TaC_{0.90}$	s,*	303	120	217	0.262		[27]

concentration and porosity) and purity of the samples used in each study.

It is also useful to compare the corrected elastic moduli of the transition-metal carbide ceramics with the Hill averages of the Voigt and Reuss polycrystalline approximations calculated from the SOECs (C_{11}, C_{12} and C_{44}) of single-crystal samples (Table III). This technique of approximating SOECs to the technological elastic moduli of isotropic polycrystalline materials is commonly used to compare the measured elastic moduli data of ceramics with those of single crystals. Only limited experimental data are available for the SOECs of transition-metal carbide single crystals at room temperature, which were determined using different methods. Gilman and Roberts [26] and Chang and Graham [10] employed pulse-echo ultrasonics, and Pintschovius *et al*. [11] performed an inelastic neutron study to determine a complete set of SOECs for single crystal TiC. Bartlett and Smith measured the velocities of ultrasonic pulses using a double transducer technique [27] to determine the SOECs for single crystal $TaC_{0.90}$. The data for SOECs of TiC quoted in a paper by Rowcliffe and Hollox [28] were from a private communication. The Hill averages of the Voigt and Reuss polycrystalline approximations as given in Table III were calculated using standard equations (see for instance [29]). The equations for the upper (μ_V, Voigt) and lower (μ_R, Reuss) bounds of the shear stiffness and bulk modulus, for cubic crystals, take the form:

$$\mu_V = (C_{11} - C_{12} + 3C_{44})/5, \tag{2}$$

$$\mu_R = \frac{5(C_{11} - C_{12})C_{44}}{4C_{44} + 3(C_{11} - C_{12})}, \tag{3}$$

$$B_V = B_R = (C_{11} + 2C_{12})/3. \tag{4}$$

The Young's modulus bounds can be calculated from Equations 2 to 4 using

$$E_{V,R} = \frac{9B_{V,R}\mu_{V,R}}{3B_{V,R} + \mu_{V,R}}. \tag{5}$$

The Young's, shear and bulk moduli and Poisson's ratio for the $TiC_{0.98}$ and $TaC_{0.98}$ ceramic samples, which were corrected for the effects of porosity, are in reasonable agreement with the corresponding Hill averages of the Voigt and Reuss polycrystalline approximations (Table III). Williams and Schaal [30] determined the Young's modulus (E) of single-crystal $TiC_{0.94}$ from experimental stress-strain curves in the ⟨100⟩ crystallographic direction. The result of this study produced $E = 448 \pm 40$ GPa for single-crystal $TiC_{0.94}$, which is in good agreement with the porosity corrected value found in this study for ceramic $TiC_{0.98}$.

The bulk modulus of transition-metal carbides, in particular that of TiC, has been the subject of several experimental and theoretical investigations. Apart from the aforementioned experimental studies on polycrystalline samples, a high-pressure X-ray diffraction study [31] yielded a bulk modulus value of 235 ± 2 GPa for cubic TiC at room temperature and atmospheric pressure (but the actual carbon concentration of the sample was not specified). The present result for the adiabatic bulk modulus of the non-porous matrix of ceramic $TiC_{0.98}$ (Table III) is in good agreement with this value. Considerable effort has been devoted to the determination of the bulk modulus of transition-metal carbides from model calculations. In studies on stoichiometric TiC, Zhukov *et al*. [32] used the linear muffin-tin orbitals method (LMTO) and atomic spheres approximation (ASA) to produce a value of 394 GPa, while Price *et al*. [33] produced 310 GPa using full potential (FP) LMTO study. Guemmaz *et al*. [34] also used FP-LMTO method to generate a bulk modulus of 220 GPa. Values of 357, 242, and 246 GPa were deduced by Jochym *et al*. [35] from *ab-initio* calculations involving the determination of the slope of acoustic-mode dispersion curves, deformation energy, and stress-strain relations, respectively. Total energy calculations using full potential linear augmented plane wave (FP-LAPW) and the general gradient approximation (GGA) were employed by Méçabih *et al*. [36] and a value of 273 GPa was found for the bulk modulus of TiC. Ahuja *et al*. [37] determined two values for the bulk modulus of TiC, 270 and 220 GPa using local density approximation (LDA) and GGA, respectively, within density functional theory. From first-principles calculations of elastic and thermal properties Wolf *et al*. [29] obtained 286 GPa for the bulk modulus of single-crystal TiC.

In general, the elastic property least affected by porosity is Poisson's ratio; the ranges of values quoted by Kral *et al*. [9] for nearly stoichiometric transition-metal carbides are 0.17–0.19 and 0.19–0.24, for TiC and TaC, respectively. The values of Poisson's ratio of the carbide ceramics determined in this study (see Tables II and III) fall into the ranges mentioned above. The acoustic Debye temperatures for ceramic $TiC_{0.98}$ and $TaC_{0.98}$ (Table III), calculated using the ultrasonic velocity values corrected for the effects of porosity, fall in the ranges quoted by [38]: 845–950 K for TiC and 573–616 K for TaC.

The variations of longitudinal (C_L) and shear (μ) elastic stiffnesses with temperature for each carbide are shown in Fig 2a and b, respectively. They were obtained from the sample density and the measured velocities of 30 MHz ultrasonic waves propagated in the ceramic sample as it was cycled between room temperature and the lowest temperature of measurements. There was no measurable thermal hysteresis in the ultrasonic wave velocities and no irreversible effects. Corrections on elastic moduli for sample length and density changes are expected to be negligible due to the low thermal expansion of these carbides [1, 39, 40]. Both the longitudinal and shear stiffnesses of the $TiC_{0.98}$ and $TaC_{0.98}$ ceramics increase with decreasing temperature and do not show any pronounced unusual effects. The temperature dependencies of both C_L and μ can be approximated by a conventional lattice vibrational anharmonicity model [41], represented by the dashed lines through the experimental data points in Fig 2a and b. For ceramic $TiC_{0.98}$, this elastic behaviour with temperature is in accord with single-crystal elastic constants as functions of temperature [10], in the sense that the elastic stiffness moduli stiffen upon cooling.

The variation of Young's modulus with temperature for the $TiC_{0.98}$ and $TaC_{0.98}$ ceramics is shown in Fig. 2c. The increase in Young's modulus with decreasing temperature is in accord with and complement those found previously in the temperature range 20–1600°C for TiC [5] and 300–2300 K for TaC [6, 7]. Fig. 2d shows the temperature dependence of the adiabatic bulk modulus of these carbides. The bulk modulus of each carbide ceramic shows approximately linear temperature dependence over the measured temperature range. A linear increase in bulk modulus with decreasing temperature was observed for a $TaC_{0.99}$ sample [7], which is in accord with that found here for the $TaC_{0.98}$ ceramic. No data for the temperature dependence of the bulk modulus of ceramic $TiC_{0.98}$ is available in the literature. Poisson's ratio for each of the $TiC_{0.98}$ and $TaC_{0.98}$ ceramics decreases very slightly with decreasing temperature. The acoustic Debye temperature for both ceramics increases slightly on decreasing temperature, in line with the increased stiffness under cooling.

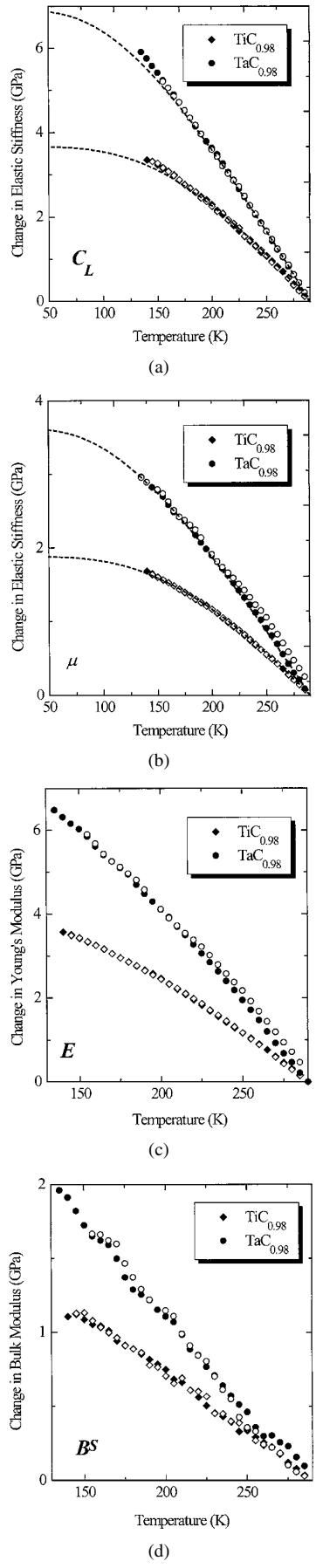

Figure 2 The change in elastic modulus with temperature ($M(T) - M(290\ K)$): (a) longitudinal stiffness, (b) shear stiffness, (c) Young's modulus and (d) bulk modulus. The filled (open) symbols correspond to measurements made with decreasing (increasing) temperature. The dashed lines refer to the elastic moduli calculated by fitting the lattice vibrational anharmonicity model [41] to the experimental data.

4. Hydrostatic pressure dependences of the ultrasonic wave velocity and elastic stiffness moduli

The effects of hydrostatic pressure on ultrasonic wave velocity in the $TiC_{0.98}$ and $TaC_{0.98}$ ceramics are shown

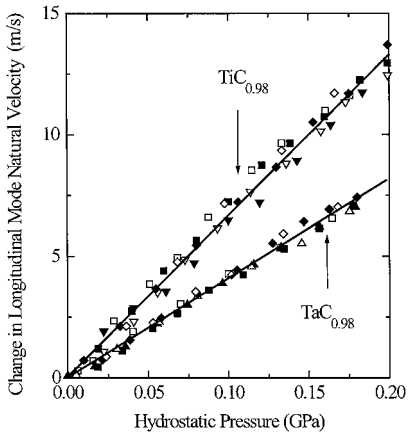

(a)

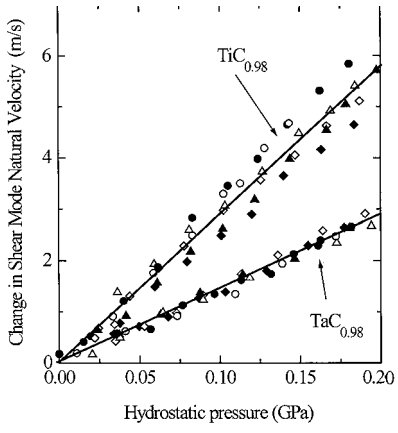

(b)

Figure 3 Hydrostatic pressure dependence of the change in natural velocity for (a) the longitudinal mode and (b) the shear mode, measured at room temperature. The filled symbols correspond to measurements made with increasing pressure and the open symbols to data as the pressure was decreased (different symbols refer to different experimental runs). The straight lines are the least-squares fits to the experimental data.

in Fig 3a and b for the longitudinal and shear modes, respectively. The data for the pressure dependence of the velocities of both longitudinal and shear ultrasonic waves are reproducible under pressure cycling and show no measurable hysteresis effects. This observation indicates that both the $TiC_{0.98}$ and $TaC_{0.98}$ ceramics do not alter in morphology under pressure cycling up to 0.2 GPa and that there is no relaxation of any residual stress. The longitudinal mode velocity is much more pressure dependent than that of the shear mode. The velocities of both the longitudinal and shear ultrasonic waves increase approximately linearly with pressure. This is a normal behaviour: both the long-wavelength longitudinal and shear acoustic modes stiffen under pressure. No indication of mode softening in the measured pressure range was found.

The hydrostatic pressure derivative $(\partial M/\partial P)_{P=0}$ of elastic stiffness (M) has been obtained from the ultrasonic velocity measurements under pressure by using [42]

$$\left(\frac{\partial M}{\partial P}\right)_{P=0} = (M)_{P=0}\left[\frac{2(\partial f/\partial P)}{f} + \frac{1}{3B^{T}}\right]_{P=0}. \quad (6)$$

where B^{T} is the isothermal bulk modulus, f is the pulse-echo overlap frequency at atmospheric pressure and $\partial f/\partial P$ is its pressure derivative. The adiabatic bulk modulus B^{S} has been used rather than B^{T} throughout the calculations: a procedure, which introduces only a negligible error. The hydrostatic pressure derivatives $(\partial C_{L}/\partial P)_{P=0}$, $(\partial \mu/\partial P)_{P=0}$ and $(\partial B^{S}/\partial P)_{P=0}$ determined for the $TiC_{0.98}$ and $TaC_{0.98}$ ceramics have positive values characteristic of a stiff solid (Table II). Both the longitudinal and shear elastic stiffnesses and thus the slopes of the corresponding acoustic-mode dispersion curves, at the long-wavelength limit, increase with pressure in the normal way. It is known that the porous microstructure of ceramics affects the hydrostatic pressure induced changes in ultrasonic velocities and hence the pressure derivative $(\partial B^{S}/\partial P)_{P=0}$ of the bulk modulus [43]. However, the results found for $(\partial B^{S}/\partial P)_{P=0}$ for both the $TiC_{0.98}$ and $TaC_{0.98}$ ceramics (Table II) do not seem to be greatly influenced by the porous nature of the ceramic samples.

It is instructive to compare the values obtained in this work for $(\partial B^{S}/\partial P)_{P=0}$ of $TiC_{0.98}$ and $TaC_{0.98}$ ceramics with those determined by other researchers using other methods. Dubrovinskaia *et al.* [31] performed X-ray powder diffraction measurements on cubic TiC under quasi-hydrostatic pressure conditions up to 18 GPa at room temperature and analysed the data on the pressure dependence of the unit cell volume in terms of the Birch-Murnaghan equation of state. They obtained a value of 6.5 for the pressure derivative of isothermal bulk modulus of cubic TiC. This value is larger than but comparable to that ($= 3.88 \pm 0.35$) measured here for the hydrostatic pressure derivative $(\partial B^{S}/\partial P)_{P=0}$ of the adiabatic bulk modulus of ceramic $TiC_{0.98}$. It is also worth noting that the value ($= 3.88 \pm 0.35$) determined for $(\partial B^{S}/\partial P)_{P=0}$ of ceramic $TiC_{0.98}$ is similar to the results of the theoretical calculations of the pressure derivative $\partial B/\partial P$ of the bulk modulus of single-crystal TiC. Méçabih *et al.* [36] used the FP-LAPW method and found a value of 4.30 for $\partial B/\partial P$; first-principles calculations of the elastic and thermal properties [29] yielded a value of 3.93 for TiC. This comparison indicates that porosity had only a small influence on the behaviour of ceramic $TiC_{0.98}$ under high pressure.

The measurements of the bulk modulus and its hydrostatic pressure derivative (Table III) have been used to calculate the volume compression $V(P)/V_0$ of ceramic $TiC_{0.98}$ and $TaC_{0.98}$ up to very-high pressures, using an extrapolation method based on the Murnaghan's equation of state [44] in the logarithmic form. The calculations have been performed at room temperature using the bulk modulus values corrected for the effects of porosity and the results are shown in Fig. 4. The calculated volume compression of ceramic $TiC_{0.98}$ is in reasonable agreement with that obtained from high-pressure X-ray powder diffraction measurements on TiC [31]. Fig. 4 also show that $TaC_{0.98}$ is less compressible than $TiC_{0.98}$. Previously measured data for volume compression of TaC is not available in the literature. According to Dubrovinskaia *et al.* [31], TiC undergoes a structural phase transition at 18 GPa, from cubic to rhombohedral. In contrast, Sekine and Kobayashi [45] detected no phase transition for TiC up to 200 GPa from high-pressure Hugoniot measurements.

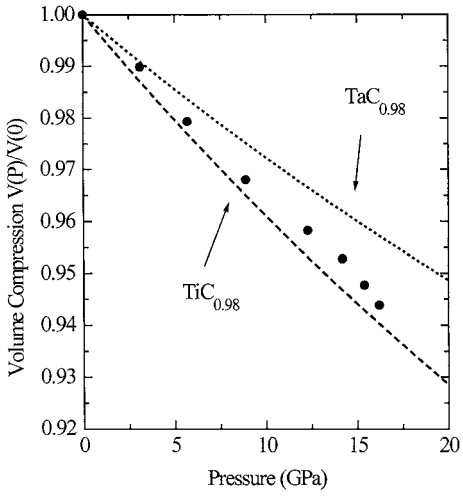

Figure 4 Volume compression of $TaC_{0.98}$ (dotted line) and $TiC_{0.98}$ (dashed line) at room temperature extrapolated to very high pressures, using Murnaghan's equation of state [44], in comparison with the high-pressure X-ray diffraction data for TiC (filled circles) [31].

5. Grüneisen parameters and acoustic mode vibrational anharmonicity

The hydrostatic pressure dependences of ultrasonic wave velocities quantify to first order the vibrational anharmonicity of long-wavelength acoustic modes. Properties of a solid that depend upon thermal motion of the atoms are much influenced by anharmonicity. Common practice is to describe the anharmonic properties in terms of Grüneisen parameters, which quantify the volume or strain dependence of the lattice vibrational frequencies. The dependence of the acoustic-mode frequency ω_p in a phonon branch p on volume V can be expressed as a mode Grüneisen parameter

$$\gamma_p = -\left[\frac{\partial(\ln \omega_p)}{\partial(\ln V)}\right]_T, \tag{7}$$

which can be obtained from the measurements of the elastic stiffnesses and their pressure derivatives. The longitudinal (γ_L) and shear (γ_S) acoustic-mode Grüneisen parameters have been determined using

$$\gamma_L = -\frac{1}{6C_L}\left[C_L - 3B^T\left(\frac{\partial C_L}{\partial P}\right)_{P=0}\right] \tag{8}$$

and

$$\gamma_S = -\frac{1}{6\mu}\left[\mu - 3B^T\left(\frac{\partial \mu}{\partial P}\right)_{P=0}\right], \tag{9}$$

respectively. The mean acoustic-mode Grüneisen parameter (γ^{el}), which is a measure of the overall contribution of zone-centre acoustic modes to the lattice vibrational anharmonicity, has been obtained using

$$\gamma^{el} = \frac{1}{3}(\gamma_L + 2\gamma_S). \tag{10}$$

This expression is strictly valid only at temperatures, which are comparable with the acoustic Debye temperature. The results obtained for γ_L, γ_S and γ^{el} of ceramic $TiC_{0.98}$ and $TaC_{0.98}$ at room temperature are included in Table II. All acoustic-mode Grüneisen parameters are positive and typical for a stiff solid. The values found for the shear γ_S of ceramic $TiC_{0.98}$ and $TaC_{0.98}$ are small and approximately the same, indicating that shear acoustic mode vibrational anharmonicity is low in these carbides. No previous experimental determination of the acoustic-mode Grüneisen parameters for these carbides has been performed. Recently, from a theoretical study on the nonlinear acoustic properties of TiC, Wolf *et al.* [29] estimated a Grüneisen parameter γ (~1.03–1.33), which is similar to γ^{el} ($= 1.11 \pm 0.08$) of ceramic $TiC_{0.98}$ determined in this work (Table II). Hence, the acoustic-mode Grüneisen parameters (γ_L, γ_S and γ^{el}) provide reasonable estimates for the contribution of the long-wavelength acoustic phonon modes to the thermal properties of $TiC_{0.98}$ and $TaC_{0.98}$.

The thermal Grüneisen parameter γ^{th} ($= 3\alpha V B^S/C_P$) quantifies the contributions of both acoustic and optical phonon modes throughout the first Brillouin zone to the thermal properties of a material. An estimate of the thermal Grüneisen parameter has been made for these carbide ceramics using the room-temperature thermal expansion (α) data [40] and specific heat (C_P) results [39]. The calculation of γ^{th} from these data and the present data for the adiabatic bulk modulus (B^S) produced the values of 1.88 and 2.34 for ceramic TiC and TaC, respectively. The relatively larger values obtained for γ^{th} in comparison to γ^{el} measured here for ceramic $TiC_{0.98}$ and $TaC_{0.98}$ implies that the optical phonons have relatively larger Grüneisen parameters. Small values for the acoustic-mode Grüneisen parameters (Table II) and hence low vibrational anharmonicities are compatible with the low thermal expansions of both TiC and TaC.

6. Conclusions

The velocities of longitudinal and shear 10–50 MHz ultrasonic waves propagated in ceramic $TiC_{0.98}$ and $TaC_{0.98}$ have been measured as functions of temperature and hydrostatic pressure. There are several interesting features to note, which shed light on the elastic, nonlinear acoustic and lattice dynamical properties of these transition-metal carbides. They can be summarised as follows:

1. The ceramic $TiC_{0.98}$ and $TaC_{0.98}$ are comparatively stiff materials elastically. The volume-dependent elastic stiffness (C_L) and the adiabatic bulk modulus (B^S) of each ceramic are large. The bulk modulus of $TiC_{0.98}$ and $TaC_{0.98}$ is in accord with the strong interatomic bonding in these materials. The shear stiffness (μ) of each of the $TiC_{0.98}$ and $TaC_{0.98}$ ceramics is also large, indicating that these ceramics have a large resistance to applied shear stress.

2. Both the longitudinal and shear stiffnesses of ceramic $TiC_{0.98}$ and $TaC_{0.98}$ show normal behaviour with temperature and can be fitted to the conventional model for vibrational anharmonicity. The bulk and Young's moduli of these carbides increase with decreasing temperature and do not show any unusual effects.

3. The hydrostatic pressure derivatives of the longitudinal and shear elastic stiffnesses and that of the bulk modulus for ceramic $TiC_{0.98}$ and $TaC_{0.98}$ have positive values, which are characteristic of a stiff solid.

4. The long-wavelength longitudinal, shear and mean acoustic-mode Grüneisen parameters determined for ceramic $TiC_{0.98}$ and $TaC_{0.98}$ are small and positive. The thermal properties of these ceramics are in accord with the low acoustic-mode vibrational anharmonicity. The values obtained for the thermal Grüneisen parameter of ceramic $TiC_{0.98}$ and $TaC_{0.98}$ are larger when compared to their mean acoustic-mode Grüneisen parameters indicating that optical phonons in these carbides have relatively larger mode Grüneisen parameters.

Acknowledgments

We would like to thank Professor G. A. Saunders for his continuous support during the work, and E. F. Lambson, W. A. Lambson and R. C. J. Draper for technical assistance. B. J. is grateful to MOD for Corporate Research Programme funding.

References

1. L. E. TOTH, "Transition Metal Carbides and Nitrides" (Academic Press, New York, 1971).
2. W. S. WILLIAMS, *J. Min. Met. Mater. Soc.* **49** (1997) 38.
3. W. S. WILLIAMS in "Science of Hard Materials 3," edited by V. K. Sarin (Elsevier Applied Science, London, 1988).
4. W. S. WILLIAMS, *Int. J. Refract. Met. & Hard Mater.* **17** (1999) 21.
5. R. H. J. HANNINK and M. J. MURRAY, *J. Mater. Sci.* **9** (1974) 223.
6. V. G. BUKATOV, O. S. KOROSTIN and V. I. KNYAZEV, *Inorg. Mater.* **11** (1975) 313.
7. C. K. JUN and P. T. B. SHAFFER, *J. Less-Common Metal.* **23** (1971) 367.
8. H. L. BROWN, P. E. ARMSTRONG and C. P. KEMPTER, *J. Chem. Phys.* **45** (1966) 547.
9. C. KRAL, W. LENGAUER, D. RAFAJA and P. ETTMAYER, *J. Alloys Comp.* **265** (1998) 215.
10. R. CHANG and L. J. GRAHAM, *J. Appl. Phys.* **37** (1966) 3778.
11. L. PINTSCHOVIUS, W. REICHARDT and B. SCHEERER, *J. Phys. C: Solid State Phys.* **11** (1978) 1557.
12. E. K. STORMS, "Refractory Carbides" (Academic Press, New York, 1968).
13. M. DESMAISON-BRUT, N. ALEXANDRE and J. DESMAISON, *J. Eur. Ceram. Soc.* **17** (1997) 1325.
14. D. R. LIDE (ed.), "Handbook of Chemistry and Physics" (75th edn., CRC Press, London, 1994).
15. M. YAMASHITA, *J. Phys. E: Sci. Instrum.* **20** (1987) 1457.
16. C. C. WANG, S. A. AKBAR, W. CHEN and V. D. PATTON, *J. Mater. Sci.* **30** (1995) 1627.
17. F. A. MODINE, M. D. FOEGELLE, C. B. FINCH and C. Y. ALLISON, *Phys. Rev.* B **40** (1989) 9558.
18. E. P. PAPADAKIS, *J. Acoust. Soc. Amer.* **42** (1967) 1045.
19. E. KITTINGER, *Ultrasonics* **15** (1977) 30.
20. R. N. THURSTON and K. BRUGGER, *Phys. Rev.* **133** (1964) A1604.
21. D. L. PRICE and B. R. COOPER, *Phys. Rev.* **39** (1989) 4945.
22. P. C. WATERMAN and R. TRUELL, *J. Math. Phys.* **2** (1961) 512.
23. C. M. SAYERS and R. L. SMITH, *Ultrasonics* **20** (1982) 201.
24. Q. YANG, W. LENGAUER, T. KOCH, M. SCHREERER and I. SMID, *J. Alloys Comp.* **309** (2000) L5.
25. I. N. FRANTSEVICH, E. A. ZHURAKOVSKII and A. B. LYASHCHENKO, *Inorg. Mater.* **3** (1967) 6.
26. J. J. GILMAN and B. W. ROBERTS, *J. Appl. Phys.* **32** (1961) 32.
27. R. W. BARTLETT and C. W. SMITH, *ibid.* **38** (1967) 5428.
28. D. J. ROWCLIFFE and G. E. HOLLOX, *J. Mater. Sci.* **6** (1971) 1270.
29. W. WOLF, R. PODLOUCKY, T. ANTRETTER and F. D. FISCHER, *Phil. Mag.* B **79** (1999) 839.
30. W. S. WILLIAMS and R. D. SCHAAL, *J. Appl. Phys.* **33** (1962) 955.
31. N. A. DUBROVINSKAIA, L. S. DUBROVINSKY, S. K. SAXENA, R. AHUJA and B. JOHANSSON, *J. Alloys. Comp.* **289** (1999) 24.
32. V. P. ZHUKOV, V. A. GUBANOV, O. JEPSEN, N. E. CHRISTENSEN and O. K. ANDERSEN, *J. Phys. Chem. Solids* **49** (1988) 841.
33. D. L. PRICE, B. R. COOPER and J. M. WILLS, *Phys. Rev.* B **46** (1992) 11368.
34. M. GUEMMAZ, A. MOSSER, R. AHUJAB and B. JOHANSSON, *Sol. St. Comm.* **110** (1999) 299.
35. P. T. JOCHYM, K. PARLINSKI and M. STERNIK, *Eur. Phys. J.* B **10** (1999) 9.
36. S. MÉÇABIH, N. AMRANE, Z. NABI, B. ABBAR and H. AOURAG, *Physica* A **285** (2000) 392.
37. R. AHUJA, O. ERIKSSON, J. M. WILLS and B. JOHANSSON, *Phys. Rev.* B **53** (1996) 3072.
38. Y. A. CHANG, L. E. TOTH and Y. S. TYAN, *Metall. Trans.* **2** (1971) 315.
39. A. KRAJEWSKI, L. D'ALESSIO and G. DE MARIA, *Cryst. Res. Technol.* **33** (1998) 341.
40. H. STUART and N. RIDLEY, *J. Iron. St. Inst.* **208** (1970) 1087.
41. S. C. LAKKAD, *J. Appl. Phys.* **42** (1971) 4277.
42. R. N. THURSTON, *Proc. IEEE* **53** (1965) 1320.
43. Q. WANG, G. A. SAUNDERS, D. P. ALMOND, M. CANKURTARAN and K. C. GORETTA, *Phys. Rev.* B **52** (1995) 3711.
44. F. D. MURNAGHAN, *Proc. Natl. Acad. Sci. USA* **30** (1944) 244.
45. T. SEKINE and T. KOBAYASHI, *J. Mater. Proc. Technol.* **85** (1999) 11.

Received 21 October
and accepted 25 November 2002